J. Serb. Chem. Soc. 91 (0) 1–24 (2026)
JSCS–13713

Original scientific paper
Published XX M 2026

Fabrication of chitosan membrane modified by vanillin and gelatin for crystal violet dye adsorption

KHABIBI KHABIBI*, NABILA AMALIA IZAAZ AANISA and RETNO ARIADI LUSIANA

Department of Chemistry, Faculty of Sciences and Mathematics, University of Diponegoro 50275 Semarang, Central Java, Indonesia

(Received 9 January, revised 27 January, accepted 9 April 2026)

Abstract: Crystal violet is a cationic dye that poses serious environmental risks when accumulated in aquatic ecosystems due to its high toxicity to living organisms. Therefore, effective treatment methods are required to remove this dye from wastewater. In this study, a chitosan (Cs)-based bioadsorbent membrane, cross-linked with vanillin (V) and modified with gelatin (G), was developed to adsorb crystal violet dye. The chitosan/vanillin membrane was mixed with gelatin at various concentrations of 0.5 (CsVG1), 0.75 (CsVG2) and 1 % (CsVG3). The adsorption process was examined as a function of pH, contact time, initial dye concentration and temperature. Physicochemical characterization of the membranes included porosity, swelling degree, water absorption, FTIR and SEM analysis. The results showed that the optimal parameters for dye adsorption were pH 6, contact time of 80 min, and temperature of 298 K, resulting in 88 % dye removal. The adsorption kinetics followed a pseudo-second-order model and the Freundlich model best described the adsorption isotherm. The thermodynamic analysis demonstrated that the adsorption process was spontaneous and exothermic. Thus, the CsVG membrane has the potential to serve as an effective alternative for removing crystal violet from textile industrial wastewater.

Keywords: biopolymers; bioadsorbent; adsorption membrane; dye removal.

INTRODUCTION

Industrial waste containing synthetic dyes poses substantial risks to environmental integrity and public health. Dyes in water can reduce light penetration and lower dissolved oxygen levels, disrupting the photosynthesis of aquatic organisms. Furthermore, these dyes have the potential to cause carcinogenic and mutagenic consequences in aquatic creatures and humans.[1] It is estimated that approximately 800,000 t of dyes are produced each year, of which about 20 % are discharged into water bodies at the final stage of industrial processes.[2] One type of synthetic dye

* Corresponding author. E-mail: khabibi@live.undip.ac.id
https://doi.org/10.2298/JSC260109020K

that is widely used is cationic dyes, such as crystal violet. The chemical composition of these dyes is characterized by a complex, highly stable aromatic structure, which renders them difficult to degrade naturally.[3] Crystal violet can significantly reduce the amount of light that passes through and alter the appearance of water, even at low concentrations.[4] Given these challenges, recent research highlights the importance of developing practical, environmentally friendly ways to remove these dangerous compounds.

Various waste treatment methods have been developed, such as adsorption, flocculation, membrane filtration, photocatalysis and ion exchange.[5,6] Among these technologies, adsorption is a viable approach for dye waste treatment owing to its high efficacy, cost-effectiveness and operational simplicity. The choice of adsorbent material significantly influences the adsorption process; however, traditional adsorbents, such as commercial activated carbon, have drawbacks including elevated production and regeneration costs, limited selectivity, and reduced reusability.

To improve the efficiency of the adsorption process, bio-based materials are a promising alternative because they are simple, effective and utilize renewable resources. The increasing demand for environmentally friendly processing technologies has encouraged the use of natural biopolymers as efficient adsorbents. Recent studies show that biopolymers such as cellulose, chitin and chitosan are gaining attention for dye adsorption applications due to their abundance, affordability and customizable properties, including surface area, pore size and volume, ease of modification and environmental sustainability.[7] The review also confirms that chitosan is a superior candidate material as a membrane base for effective dye removal in wastewater treatment.

Chitosan is a biopolymer produced by the deacetylation of chitin extracted from marine crustaceans, formed from basic structural units of amino glucose and *N*-acetyl amino glucose connected by β-1,4-glycosidic bonds.[8] Chitosan-based adsorbents are effective for dye adsorption owing to their high surface area, numerous functional groups and good biocompatibility. Chitosan contains numerous amino and hydroxyl groups, which are crucial for its interaction with dyes.[9,10] Chitosan's solubility in acidic solutions and its limited mechanical strength necessitate physical and chemical modifications to improve stability and adsorption efficiency.[11] Vanillin is a phenolic aldehyde that can serve as a natural cross-linking agent due to its non-toxic properties and its ability to enhance the mechanical properties of chitosan membranes, thereby offering a safer alternative to synthetic cross-linking agents such as glutaraldehyde.[11] Gelatin is a mixture of peptides and proteins produced from the controlled hydrolysis of collagen. Gelatin has a high adsorption capacity due to the presence of hydroxyl, carboxyl and amino groups along its molecular chain,[12] thereby increasing the number of active sites on the membrane for dye adsorption.

In this study, vanillin-crosslinked chitosan membranes were synthesized *via* a Schiff base modification reaction on chitosan, then combined with gelatin to increase the number of active sites on the membrane surface during dye removal from aqueous solutions. The chitosan/vanillin/gelatin (CsVG) membrane was characterized to determine its physicochemical properties using swelling degree tests, Fourier transform infrared spectroscopy (FTIR), scanning electron microscopy (SEM) and X-ray diffraction (XRD). Crystal violet was used as a model toxic cationic dye to assess the adsorption capacity of the CsVG membrane. The adsorption mechanism, isotherm model, kinetics and thermodynamic parameters were also analyzed to understand the interaction process between the dye and the membrane. The novelty of this research is that there are no reports in the literature describing the use of modified chitosan, vanillin and gelatin biopolymers as adsorbent membranes for the removal of crystal violet dye. The development of CsVG membranes as adsorbent membranes is expected to be a promising technology for effective, environmentally friendly dye removal from wastewater.

EXPERIMENTAL

Materials

The materials used in this study were chitosan (*MW* = 40,000 g/mol, *DD* = 88.5 %, Cv. Bio Chitosan Indonesia), CH_3COOH (*MW* = 131.11 g/mol, Merck), NaOH (*MW* = 40 g/mol, Merck), vanillin (*MW* = 152.15 g/mol, Merck), gelatin (Merck), crystal violet ($C_{25}H_{30}C_lN_3$, *BM*= 407.98 g/mol, Merck), HCl, (37 %, Merck) and distilled water.

Synthesis of chitosan membrane

1.5 g of chitosan was dissolved in 100 mL of 1 % acetic acid. The solution was stirred continuously for 24 h at room temperature. The resulting chitosan solution was poured into a Petri dish and dried at 40–50 °C. The chitosan membrane was immersed in 1 M NaOH, washed with distilled water and then dried.

Synthesis of chitosan/vanillin/gelatin (CsVG) membrane

Chitosan (1.5 g) was dissolved in 60 mL of 1 % acetic acid solution with stirring for 24 h at room temperature. Separately, vanillin (0.5 g) was dissolved in 100 mL of 1 % acetic acid and stirred for 2 h at 50 °C. The gelatin solution was prepared by dissolving gelatin in 100 mL of distilled water at 50 °C with agitation for 2 h, at concentrations of 0.5 (CsVG1), 0.75 (CsVG2) and 1 % (CsVG3). The chitosan solution was subsequently combined with 20 mL of vanillin solution and agitated for 4 h at 60 °C to facilitate cross-linking reactions. Next, the gelatin solution was added to the chitosan–vanillin mixture, and stirring was continued for 24 h until a homogeneous solution was formed. The resulting solution was then poured into Petri dishes and dried at 50 °C until a membrane was formed. The preparation process of the CsVG membrane is illustrated in Fig. 1.

Characterization of membrane

All CS, CS/Van, and Cs/Van/Gel (CsVG) membranes were characterized using various analytical techniques. Fourier-transform infrared (FTIR) spectra were recorded in the range of 4000–400 cm^{-1} at a resolution of 1 cm^{-1} resolution with 25 scans per measurement using a Shimadzu FTIR spectrometer to identify changes in functional groups and the formation of new

bonds. The crystal structure was analyzed using X-ray diffraction (XRD) using a Rigaku Mini-flex 600 instrument with CuKα radiation over a 2θ range of 3–70° scanning angle with a step size of 0.02° and a scan rate of 1° min. Dye concentrations were analyzed using a UV–Vis spectrophotometer (Shimadzu UV-1280, serial No. A120660) at the maximum wavelength of each dye. Surface morphology images were obtained using a scanning electron microscope (SEM, Thermo Scientific Quattro S).

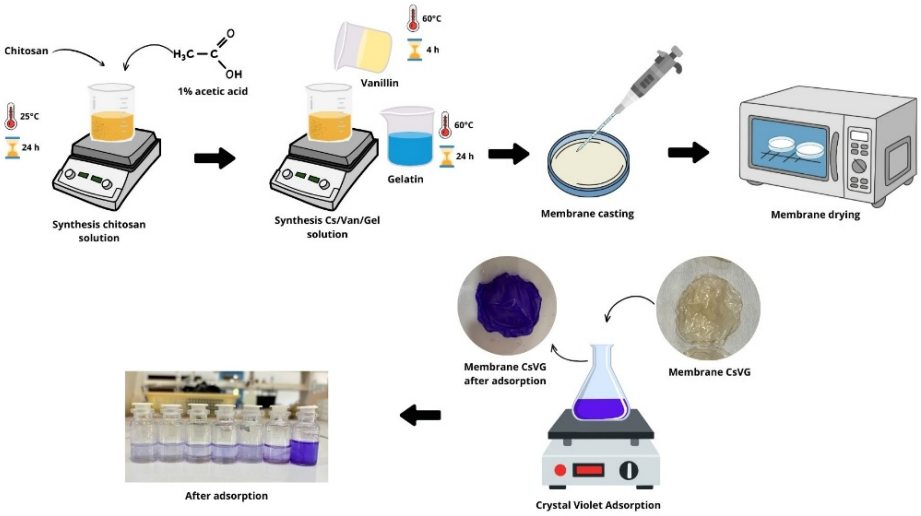

Fig. 1. Schematic diagram illustrating the preparation and dye adsorption processes of a Cs/Van/Gel membrane.

Point of zero charge (pzc)

The pHpzc of the membrane was determined through the pH shift method. 50 mL of a 0.1 M NaCl solution was prepared for the experiment. The pH of the solution was adjusted to range from 2 to 12 using 0.1 mol NaOH and 0.1 mol HCl. Each solution received 0.05 g of membrane and was allowed to stabilize for 24 h. The final pH value was recorded. The pHpzc value was determined by plotting ΔpH against pH_i and identifying the point at which ΔpH equaled zero. ΔpH can be calculatedas:

$$\Delta pH = pH_i - pH_f \quad (1)$$

where pH_i is and pH_f are initial and final pH, respectively.[13]

Physical characteristics of membranes

The membrane porosity was determined by the gravimetric method at room temperature and neutral pH. The membrane's initial weight was measured, and it was then immersed in water for 24 h. The immersed membrane was removed from the water, excess water was removed by draining on tissue paper, and it was weighed again. For each membrane, the test was repeated three times, and the porosity value was calculated using Eq (2)

$$\text{Porosity} = 100\frac{w_w - w_d}{V_m \rho_w} \quad (2)$$

where w_d is the dry membrane mass (g), w_w is the wet membrane mass after being immersed in distilled water for 24 h (g), V_m is the membrane volume (cm^3) and ρ_w is the density of water (1 g/cm^3).[14]

To determine the degree of swelling in water, the membrane was measured for its initial and final diameters after immersion in water for 24 h. The test was conducted three times. The swelling ratio was calculated using Eq. (3), where l_w is the wet membrane diameter after immersion (cm) and l_d is the dry membrane diameter (cm):[15]

$$\text{Swelling} = 100\frac{l_w}{l_d} \tag{3}$$

Water absorption was calculated from the dry membrane weight and the membrane weight after 5 h of soaking. Every hour, the membrane was dried and then weighed. Eq. (4) shows the relationship between the wet membrane and the dry membrane mass used to determine the water uptake value:[16]

$$\text{Water uptake} = 100\frac{w_w - w_d}{w_d} \tag{4}$$

Dye adsorption study

The adsorption test was based on the work by Farasati Far.[17] To make a 1000 mg/L stock solution of crystal violet, 1 g of dye was dissolved in 1 L of distilled water until fully dissolved. The initial test was conducted using 50 mL of a 5 mg/L dye solution, with a contact time of 2 hours, a solution temperature of 25 °C, and a pH ranging from 4.0 to 8.0 adjusted by adding HCl (0.01 M) and NaOH (0.01 M). The dye solution and membrane were placed in an Erlenmeyer flask and stirred with a shaker at 150 rpm. After that, 5 mL of the dye solution was taken, and its absorbance was measured at 591 nm. The test continued with different settings, including contact time (20, 60, 80, 100 and 120 min), initial dye concentration (3, 5, 7, 9 and 12 mg/L) and temperature (25, 35 and 45 °C). We systematically tested these parameters to determine the optimal conditions for crystal violet adsorption. The dye removal efficiency was determined using Eqs. (5) and (6):

$$q = \frac{c_i - c_t}{c_i}V \tag{5}$$

$$RE\% = 100\frac{c_i - c_t}{c_i} \tag{6}$$

Re% is the removal efficiency, c_i and c_t (mg/L) are the initial and final concentrations or equilibrium concentrations of the cationic dye crystal violet, V is the solution volume (L), and w is the mass of adsorbent (g).

Adsorption kinetics

The adsorption kinetics of the crystal violet dye were analyzed to understand the rate and mechanism of adsorption. The kinetic study was conducted using two commonly used models: first-order and second-order.

Pseudo-first order kinetics

This analysis is based on the principle that the adsorption rate is directly proportional to the difference between the maximum adsorption capacity and the amount of dye adsorbed at a given time. Linear and non-linear forms of the pseudo-first-order model were used.[18]

Pseudo-second-order kinetics

The pseudo-second-order kinetic model indicates that the adsorption process is influenced by intricate interactions, such as chemical bonding or the involvement of adsorption sites, suggesting a slow equilibrium system, particularly at elevated concentrations of the substance.[19] The linear and non-linear forms of the pseudo-second-order model were used.

Adsorption isotherm

An adsorption isotherm is an adsorption phenomenon that occurs at a constant temperature. The adsorption isotherm was studied using the Langmuir[20] and the Freundlich[21] models.

Thermodynamics of adsorption

The effect of temperature on dye adsorption was investigated to evaluate the thermodynamics of adsorption. Thermodynamic parameters such as Gibbs energy change (ΔG), enthalpy change (ΔH) and entropy change (ΔS) can be calculated to provide a comprehensive understanding of the adsorption process.[22] Analysis of thermodynamic parameters is useful for analyzing the nature of adsorption interactions and the stability of the complexes formed.[23]

RESULTS AND DISCUSSION

Preparation of Cs/Van/Gel (CsVG) membrane

The polymer chain of chitosan, a cationic polysaccharide, has a high density of hydroxyl and amino groups.[10] A positively charged ammonium group ($-NH_3^+$) was created by protonating the amino groups in chitosan after it was dissolved in acetic acid for this investigation. To enhance the membrane's properties, it was modified *via* vanillin cross-linking. The mechanism of the cross-linking reaction between chitosan and vanillin involves two different stages. The first stage involves the aldehyde group of vanillin reacting with the amine group of chitosan to form a Schiff base and an imine group. The imine group indicates that chitosan has been successfully cross-linked with vanillin. The covalent bonds formed during cross-linking can increase the membrane's mechanical strength. During the second stage, hydrogen bonds form between the hydroxyl group of vanillin and the hydroxyl group of chitosan or gelatin, thereby enhancing hydrophilicity and fostering a more organized structure.[25] Gelatin is subsequently incorporated *via* mixing to enhance the membrane's active sites. The $-NH_3^+$ group on protonated chitosan interacts with the carboxylate group on gelatin, which is often negatively charged in solution, thus generating electrostatic interactions.[26] The functional groups on chitosan and gelatin interact with the target chemicals, establishing hydrogen bonds.

Characterization studies

FTIR Analysis. The FTIR spectrum of the membrane shown in Fig. 2 confirms that changes occur at various stages of modification. Based on Fig. 2, chitosan shows peaks at 3358 (O–H stretching) and 3293 (primary N–H), 2878 (C–H stretching with CH_2 symmetry), 1644 and 1589 (amine twin groups), 1378 (asymmetric C–H from CH_2) and 1028 cm^{-1} (C–O–C). In the Cs/VAN membrane spectrum, the peaks at 3354 and 3297 cm^{-1} shifted from the chitosan spectrum due

to the formation of hydrogen bonds between the NH_2 of chitosan and the OH of vanillin.[27] The peak at 1644 cm^{-1} in chitosan shifted to 1639 cm^{-1}, indicating C=N stretching vibrations, which indicate the formation of a Schiff base bond between the vanillin aldehyde group and the chitosan amine group.[28] The overlap of C=O stretching vibrations originating from the secondary amide group in chitosan can make C=N stretching difficult to identify in the FTIR spectrum.[29] The broad peak at 1588 cm^{-1}, assigned to N–H bending vibrations of a secondary amine, becomes weaker, indicating that some of the amine groups have been involved in the cross--linking process.[30] In addition, a peak at 1503 cm^{-1} is attributed to the benzene ring of vanillin, and a peak at 827 cm^{-1} corresponds to the bending vibration of the phenolic hydroxyl group in vanillin. This is similar to the study by Zhang,[31] in which the addition of vanillin produced a new peak at a wavelength of 1633 cm^{-1} (C=N), a shift in the absorption peak of the benzene ring from 1584 to 1586 cm^{-1}, and a peak at 857 cm^{-1} indicating the phenolic –OH group.

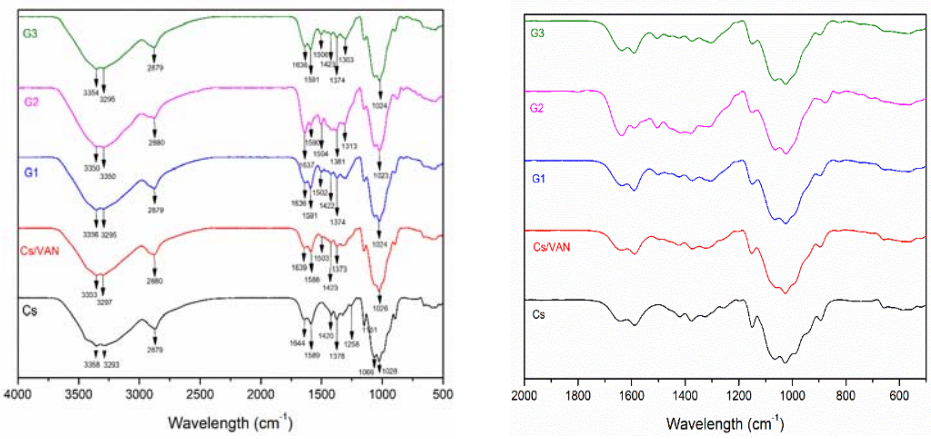

Fig. 2. FTIR spectra of Cs, Cs/VAN, G1 (Cs/Van/Gel 0.5 %), G2 (Cs/Van/Gel 0.75 %), G3 (Cs/Van/Gel 1 %) in different wavelength regions.

In the CsVG1, CsVG2, and CsVG3 membrane spectra, the OH and –NH bands shifted to lower wavenumbers because these peaks indicate intermolecular hydrogen bonds from the hydroxyl group and NH stretching from the amide group in gelatin and chitosan. At the same time, the peak at a wavelength of 1637 cm^{-1} confirms the formation of imine bonds (C=N). The C–O and C–N group peaks appear at 1024 cm^{-1}.

XRD Analysis. The XRD patterns of Cs, Cs/VAN and CsVG2 membranes are shown in Fig. 3. Pure Cs exhibits two characteristic semi-crystalline peaks at 2θ 10.89 and 20.36°,[32] which are related to the partial regularity of the polymer chain due to intra- and intermolecular hydrogen bonds between the NH_2 and OH groups.[33] The diffraction peak at about 20° became broader and less intense after

cross-linking with vanillin. It also moved to 2θ 22.29°. This change shows that chitosan and vanillin interact at the molecular level, altering the regularity of the chitosan structure. The lower intensity indicates that crystallinity has decreased because there are fewer free NH_2 groups.[34]

In the CsVG membrane, a new reflection appears at 2θ 16.99° and a peak shift from 20.36 and 22.33° and in the Cs peak shift from 22.42 to 23.39°. The shift to a higher angle indicates a decrease in *d*-spacing and the formation of a more compact polymer network through interactions among chitosan, vanillin, and gelatin.

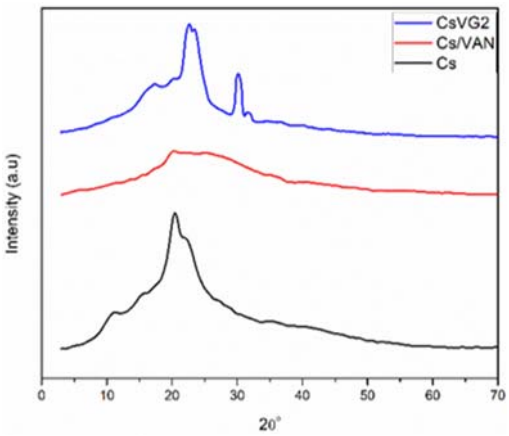

Fig 3. X-ray diffraction patterns of Cs, Cs/VAN and CsVG2 membranes.

SEM Analysis. Scanning electron microscopy (SEM) images of the Cs, Cs/VAN and CsVG membrane surfaces are shown in Fig. 4.

In Fig. 4a, SEM analysis of the chitosan membrane reveals an uneven, dense surface morphology with no visible voids, indicating reduced permeability and adsorption capacity. Fig. 4b illustrates the cross-sectional morphology of the Cs/ /VAN membrane surface, showing a smoother surface accompanied by the formation of cavities. This may be due to cross-linking, which can significantly affect the film's internal microstructure, including cavities, adhesion, smoothness and compactness. The uniformity of the pores is due to the formation of Schiff bases and hydrogen-bond interactions arising from vanillin cross-links. In Fig. 4c, the CsVG2 membrane with a gelatin concentration of 0.75 % exhibits a more consistent and smoother surface than the chitosan and chitosan/vanillin membranes, and it shows visible pores. This indicates good homogeneity among chitosan, gelatin and vanillin. The addition of gelatin to the membrane produces a smoother surface with a more homogeneous structure, thereby increasing water absorption.[35] Research by Bakouri[36] also shows that cross-sections of arginine-modified chitosan/ /gelatin films exhibit a similar dense internal structure, indicating a smooth, uniform cross-section. The more porous structure of the CsVG membrane results from

electrostatic interactions between chitosan and gelatin, which form a sponge-like structure that enhances the membrane's overall integrity.

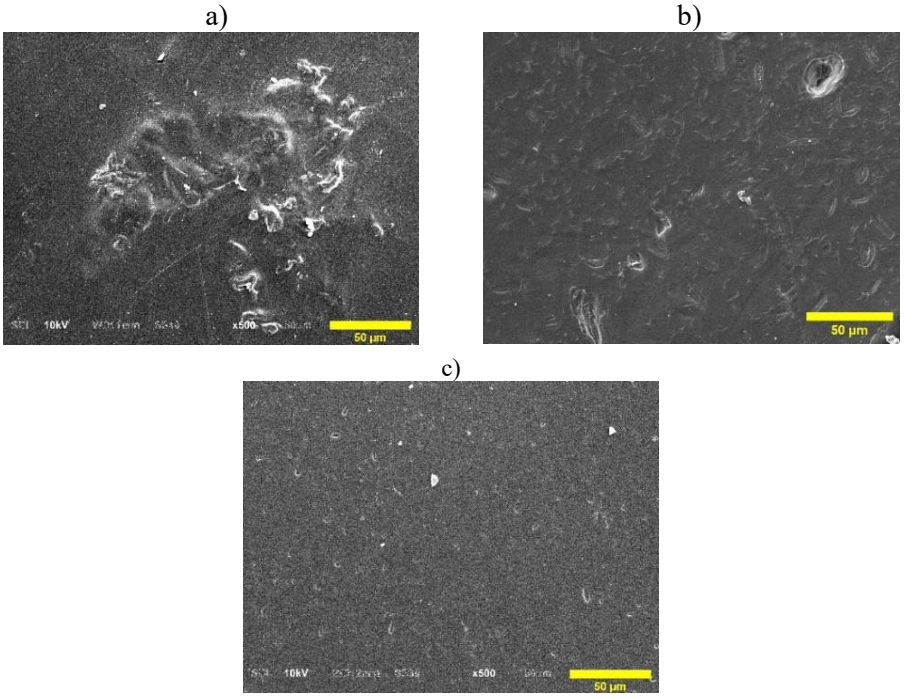

Fig. 4. SEM images at 500× magnification of: a) Cs, b) Cs/VAN and c) CsVG2 membranes after adsorption.

Point of zero charge. The point of zero charge (pHpzc) is the pH value at which the surface charge of the adsorbent is neutral.[13] At pH values below the pHpzc, Fig. 5, the adsorbent surface is positively charged, whereas at pH values above the pHpzc, it becomes negatively charged. This surface charge property plays an important role in the adsorption process because it affects the interaction between the adsorbent and the adsorbate. In this study, the cationic dye crystal

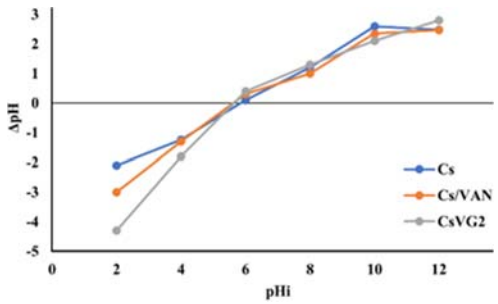

Fig. 5. pHpzc graph in the pH range 2–12.

violet (CV) was used, and it must be adsorbed at a high pH (pH > pHpzc) to achieve maximum adsorption.[37] Based on Fig. 5, the pHpzc values obtained were 5.8 for the Cs membrane and 5.6 for the Cs/VAN and CsVG2 membranes.

Physical characterization of membrane

Porosity, swelling and water uptake are critical physicochemical parameters in membranes, as they influence permeation, fouling, and polymer–water interactions, which in turn determine adsorption capacity and kinetics. The results of the physicochemical characterization of the membrane are presented in Fig. 6.

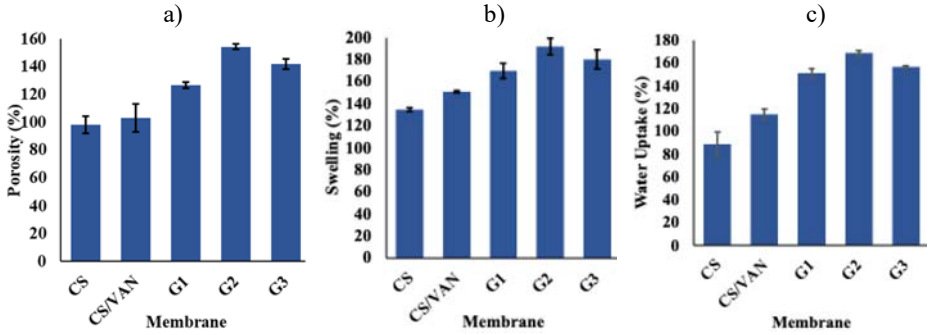

Fig. 6. a) Porosity, b) swelling degree and c) water uptake for the pure membrane and modified membranes.

To determine the effect of membrane modification with vanillin and gelatin, membrane characteristics, including porosity, degree of swelling and water absorption, were measured, as shown in Fig. 6. Fig. 6 shows that porosity, degree of swelling and water absorption increased linearly. The lowest values were obtained for the pure chitosan membrane and the physicochemical properties of the membrane increased with increasing modification levels. Among the tested variations, the CsVG2 membrane (Cs/Van/Gel 0.75 %) exhibited the best physicochemical characteristics.

Fig. 6a shows that the porosity of the pure chitosan membrane is 97.99 %, whereas that of the CsVG2 membrane it increases to 141.86 %. This indicates that increasing the gelatin concentration results in a more porous membrane structure. The presence of carboxyl groups in gelatin increases porosity through electrostatic interactions between chitosan and gelatin.[38] This increase in porosity indicates that the membrane has more empty spaces that can be filled with water, thereby increasing the internal surface area and available pore volume, which ultimately improves adsorption capacity.

The degree of swelling values in Fig. 6b indicate that the lowest swelling occurs in the pure chitosan membrane, at 134.59 %. After adding the vanillin cross-linking agent to the Cs/VAN membrane, the degree of swelling increased to

150.60 %. The addition of gelatin to the membrane significantly increased the degree of swelling. In the CsVG1 membrane, the swelling value increased to 169.78 %, and in the CsVG2 membrane with a gelatin concentration of 0.75 %, it reached 191.98 %. However, when the gelatin concentration was increased to 1 % (CsVG3 membrane), the membrane's swelling decreased to 180.01 %. The formation of cross-links between chitosan and vanillin via the Schiff base reaction produces a more compact membrane structure, reducing the number of available hydrophilic groups and thereby decreasing the membrane's swelling value.[39] However, in this study, the addition of vanillin still increased the degree of expansion. This indicates that the number of remaining hydrophilic groups is still sufficient to allow swelling, in line with the findings reported by Hu.[40]

The increase in the degree of swelling is also supported by the addition of gelatin to the chitosan matrix because gelatin has carboxyl groups that are hydrophilic and can increase the number of active groups on the membrane surface. A denser polymer network formed by stronger interactions among chitosan, vanillin, and gelatin can reduce swelling at higher gelatin concentrations. This tighter structure makes the membrane less able to absorb and expand with water, as it has less free space and fewer internal pores.

Along with the increase in porosity and degree of swelling, the percentage of water absorption shown in Fig. 6c indicates that the CsVG2 membrane has the most optimal physicochemical characteristics. A higher water-absorption capacity shows that water molecules are more strongly attracted to the membrane surface, thereby increasing the membrane's hydrophilicity. This increased hydrophilicity is critical for improving membrane performance, as it enhances its ability to absorb dyes.

Adsorption removal of crystal violet

Adsorption with variation in pH. The effect of pH on the adsorption capacity of the Cs/Van/Gel membrane was assessed by adjusting the pH of the dye solution from 4 to 8 at an initial concentration of 5 mg/L. This pH range was chosen because it represents conditions that are practically relevant for dye adsorption applications. Variations in pH are important because solution pH is a significant parameter that affects adsorption, both by altering the adsorbent surface charge and the degree of adsorbate ionization. As shown in Fig. 7, the percentage of dye removal increased with increasing solution pH from 4, reached a maximum at pH 6, and then decreased at higher pH values. Under strongly acidic conditions ($pH < 4$), chitosan may partially dissolve because of excessive protonation of amino groups, leading to structural swelling. Conversely, highly alkaline conditions can result in structural instability.

In acidic environments, the concentration of H^+ is significantly elevated, leading these ions to compete with positively charged crystal violet (CV) molecules

for negatively charged active sites on the adsorbent's surface. This condition reduces the number of sites available for CV molecules and decreases adsorption efficiency. As pH increases, the number of H^+ decreases, and the adsorbent surface tends to become negatively charged, thereby increasing electrostatic interactions with positively charged CV molecules.[41] However, when the pH is increased from 6 to 7 and 8, CV adsorption decreases. This suggests that, alongside electrostatic forces in the acidic range, mechanisms such as π–π stacking and/or hydrogen bonding are anticipated to become more prominent and potent at neutral or alkaline pH.[42,43]

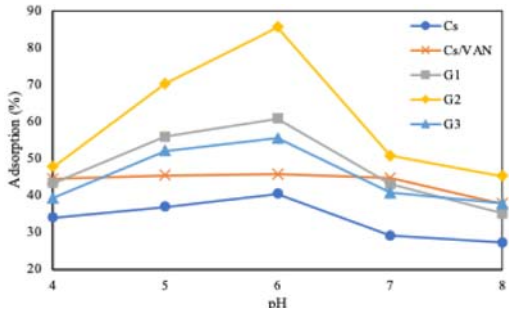

Fig. 7. Effect of pH on the CV adsorption efficiency (%); initial dye concentration, 5 mg/L, 25 °C, contact time 120 min.

At pH values above 6, adsorption efficiency decreases again, possibly due to changes in surface charge or the formation of repulsive forces between the adsorbate and adsorbent. Crystal violet is a basic dye with a pK_a value of 0.8.[44] Because of its low pK_a, this molecule remains ionized across the experimental pH range, behaving as a cationic dye under all pH conditions tested.

Adsorption with variation in time: kinetic studies. The removal of crystal violet dye by chitosan membranes and modified CsVG membranes is shown in Fig. 8. The adsorption capacity of the membrane increased until the 80th min, which facilitated greater adsorption. Subsequently, the adsorption rate decreased because most active sites were gradually filled, thereby inhibiting the diffusion of crystal violet molecules to the membrane surface. The adsorption capacity of the Cs membrane at 80 min was 35.86 %, and the maximum adsorption capacity of

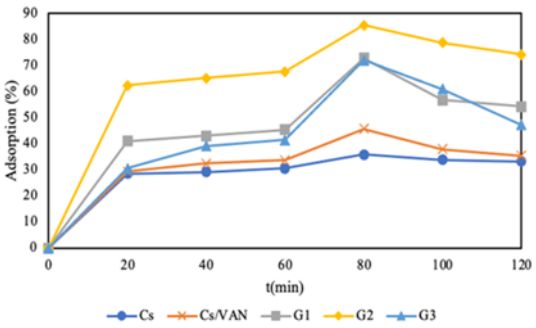

Fig. 8. Effect of contact time (min) on the CV adsorption efficiency (%); initial dye concentration, 5 mg/L; pH 6.

the CsVG2 membrane reached 85.57 %. Based on these data, the optimum adsorption time for crystal violet removal by this membrane system is 80 min.

The dye adsorption process was then analyzed using first-order and second-order pseudo-kinetic models. Adsorption kinetics provide information about the adsorption rate, the mechanism of CV adsorption by the membrane, and help determine the possible rate-controlling steps. The experimental data were analyzed using first-order and second-order pseudo-kinetic equations *via* linear and non-linear fitting. Kinetic parameters obtained from the analysis are summarized in Table I.

TABLE I. Adsorption kinetics study

Form	Plot	Parameter	Value
	Pseudo-first-order		
Linier	c_e/q_e *vs.* c_e	k_1 / min^{-1}	0.0011
		q_e / mg g^{-1}	2.3165
		R_2	0.61
		SSE	0.8653
Non-linear	q_t *vs.* t	k_1 / min^{-1}	0.074
		q_e / mg g^{-1}	1.4817
		R_2	0.9549
		SSE	0.0835
	Pseudo-second-order		
Linier	log qe vs log Ce	k_2 / g mg^{-1} min^{-1}	0.1852
		q_e / mg g^{-1}	2.3479
		R_2	0.9928
		SSE	1.4788
Non-linear	q_t *vs.* t	k_2 / g mg^{-1} min^{-1}	0.0809
		q_e / mg g^{-1}	1.6173
		R_2	0.9648
		SSE	0.065

Based on the kinetic parameters obtained from linear and non-linear regression analyses, the adsorption process is better described by the pseudo-second-order model than by the pseudo-first-order model. The pseudo-second-order model yielded higher coefficients of determination (R^2 of 0.9928 and 0.9648) than the pseudo-first-order model. Due to potential changes in the error structure resulting from linearization, model suitability was primarily assessed using nonlinear regression and *SSE* values. The pseudo-second-order model demonstrated a lower *SSE*, signifying a better fit to the experimental data. The fit of the pseudo-second-order model to the experimental data showed that the adsorption rate was controlled by the interaction between the active sites of the adsorbent and the dye molecules, where the dye-binding process involved the exchange or sharing of electron pairs between the active sites of the adsorbent and the cationic groups on the

adsorbate.[45] Other studies by Agbor Tabi[46] and Ahmad and Ejaz[47] also showed that crystal violet dye is adsorbed through chemisorption.

Adsorption with variation in initial concentration of adsorbates. The effect of the initial dye concentration on adsorption was studied by varying the concentration of crystal violet in the range of 3, 5, 7, 9 and 12 mg/L. Conversely, all other adsorption variables were kept constant, namely pH 6.0 and an adsorption time of 80 min.

Based on the results shown in Fig. 9, increasing the initial dye concentration gradually decreases the adsorption efficiency. At low crystal violet concentrations, the number of dye molecules is relatively proportional to the number of active sites available on the membrane surface, allowing CV molecules can be easily adsorbed through various interaction mechanisms, such as hydrogen bonding, electrostatic interactions, and π–π interactions between the CsVG membrane and the functional groups of crystal violet. At higher crystal violet concentrations, the number of dye molecules increases, but the number of available active sites remains limited. This discrepancy between the number of dye molecules and the number of available adsorption sites reduces the effectiveness of adsorption.[48]

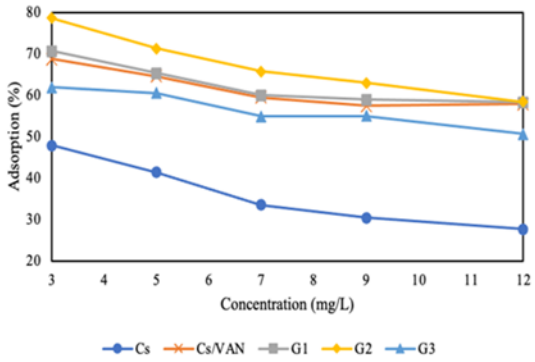

Fig. 9. Effect of dye concentration on the CV adsorption efficiency (pH 6.0; t = 80 min).

The adsorption performance of crystal violet on CsVG membranes was evaluated using adsorption isotherm studies with the Langmuir and Freundlich models. The results of the isotherm studies were used to determine the qualitative properties of the adsorbate–adsorbent systems. According to the Langmuir adsorption isotherm, adsorption occurs as a monolayer on a homogeneous surface. In contrast, the Freundlich isotherm refers to the amount of adsorbate adsorbed per unit mass of adsorbent in a heterogeneous system. The results of the CsVG membrane isotherm study are shown in Table II.

The adsorption process can be determined by the highest regression coefficient value (R^2) based on the isotherm parameters and membrane regression coefficients in Table II. The R^2 value for the Cs membrane in Langmuir is 0.9693 and in Freundlich is 0.9873, while in the CsVG2 membrane (Cs/Van/Gel 0.75 %), the

R^2 value in Langmuir is 0.9657 and in Freundlich is 0.9989. This finding suggests that the crystal violet adsorption system on all adsorbents follows the Freundlich isotherm model, as evidenced by an R^2 value exceeding the Langmuir model threshold and approaching 1. The Freundlich isotherm model assumes adsorption on a heterogeneous surface, leading to the formation of a multilayer. Additionally, the phenomenon is attributed to physical adsorption through van der Waals or weak interactions between crystal violet and the adsorbent surface.[49]

TABLE II. Isotherm adsorption study

Membrane	Langmuir			Freundlich		
	K_L	*Qmax* / mg g^{-1}	R^2	K_F / L mg^{-1}	*n*	R^2
Cs	2.6205	0.2683	0.9693	0.7796	2.1372	0.9873
Cs/VAN	8.5034	0.1633	0.8456	0.9880	1.4438	0.9896
CsVG1	8.1766	0.1823	0.854	0.8958	1.4925	0.99
CsVG2	6.0827	0.3939	0.9657	0.6103	1.8758	0.9989
CsVG3	7.8247	0.1440	0.9528	1.0899	1.3976	0.99

Adsorption with variation in temperature: thermodynamic studies. The effect of temperature on the adsorption process is shown in Fig. 10. The temperature applied in this experiment were 298, 308, 318 and 328 K. The best results were obtained with the CsVG2 membrane (Cs/Van/Gel 0.75 %), which achieved adsorption percentages of 88.12 % at 298 K and 47.33 % at 328 K. The adsorption efficiency of crystal violet decreased with increasing temperature.

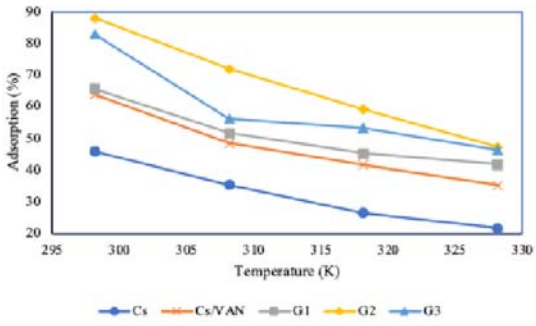

Fig. 10. Effect of temperature on the CV adsorption efficiency (pH 6.0; *t* = = 80 min: dye concentration, 3 mg/L).

The exothermic nature of the adsorption process is indicated by the decrease in adsorption capacity with increasing temperature. Thermodynamic parameters used to describe the adsorption process, such as ΔG, ΔH and ΔS, support this observation. The slope and intercept of the van't Hoff plot are used to obtain the values of $\triangle H$ and $\triangle S$. Table III presents the results of the thermodynamic parameter calculations.

According to Table III, as the temperature increases, the ΔG value indicates that the adsorption process becomes more spontaneous. The negative ΔH value

indicates that the adsorption process of crystal violet is exothermic. The Δ*S* value yields good affinity between the CsVG2 membrane and crystal violet, thereby reducing unpredictability at the solid/liquid interface during adsorption.

TABLE III. Thermodynamic parameters for CV adsorption

Membrane	Temperature, K	Δ*G* / J mol^{-1}	Δ*H* / kJ mol^{-1}	Δ*S* / J mol^{-1} K^{-1}
Cs	298.15	–201	–32.86	–111
	308.15	–1489		
	318.15	–2684		
	328.15	–3490		
CsVG2	298.15	–4229	–48.98	–150
	308.15	–2429		
	318.15	–1001		
	328.15	–291		

Interactions between CsVG membrane and the adsorbates

The adsorption mechanism depends on the functional groups and surface porosity of the adsorbent and the adsorbate molecules. An estimate of the mechanism by which the membrane-bound active groups interact with crystal violet is shown in Fig. 11.

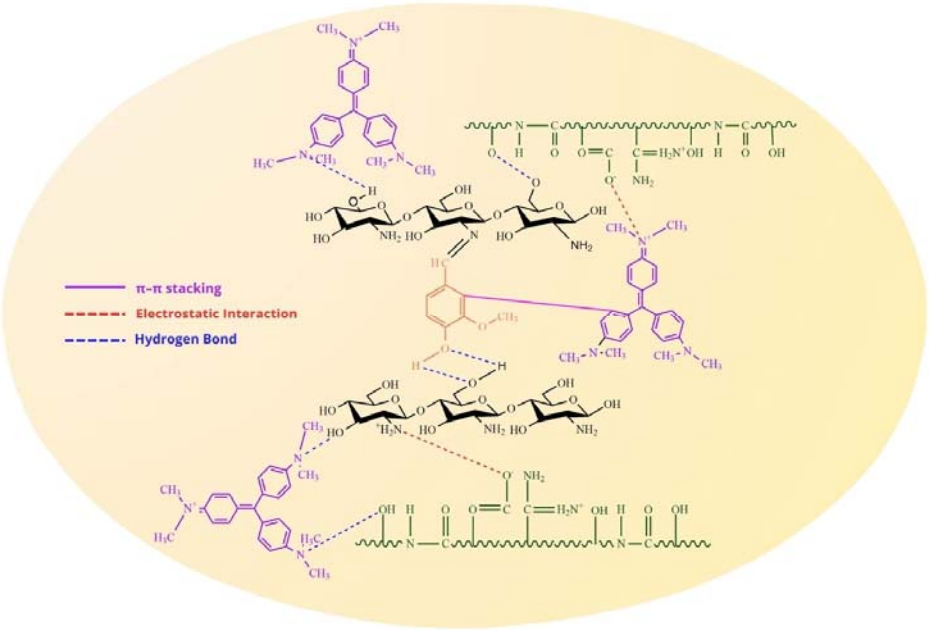

Fig. 11. Estimated adsorption mechanism.

Possible interreaction mechanisms between the active sites on the surface of the chitosan/vanillin/gelatin membrane and crystal violet include electrostatic interactions, π–π interactions and hydrogen bonding. Electrostatic bonds occur between the negative charge of the $–COO^-$ group in gelatin and the positive group (N^+) in crystal violet. The hexagonal structure of vanillin and the benzene ring of crystal violet can enhance adsorption by acting as electron donors and acceptors *via* π–π stacking. In addition, H atoms from oxygen-containing functional groups on the surface of the CsVG membrane can form hydrogen bonds with N atoms in crystal violet.

Reusability study

Reusability and stability are important parameters in evaluating the performance of adsorbents for water treatment. Therefore, the Cs and CsVG2 membranes were retested at the optimum pH for three consecutive adsorption cycles. Based on Fig. 12, the initial use showed the highest adsorption efficiency. After three cycles, the CsVG2 membrane still maintained a fairly high adsorption capacity, although the efficiency of crystal violet (CV) adsorption decreased from 89 to 49 %. This reduction in efficiency is probably caused by some CV molecules being strongly bound to active sites *via* electrostatic interactions, π–π interactions or hydrogen bonds. As a result, the number of available active sites is reduced. In addition, pore blocking by residual dye molecules may occur, inhibiting the diffusion of adsorbates into the membrane structure. This decrease indicates that optimization of the regeneration method is still needed to improve membrane reuse performance.

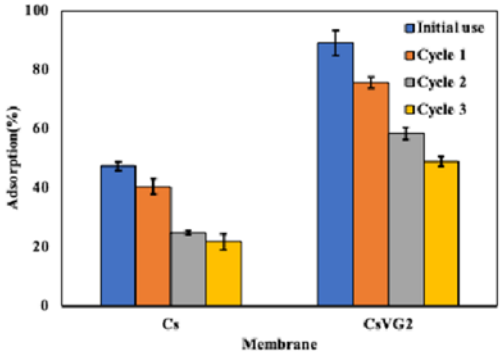

Fig. 12. The cycles of reusability of the membrane.

CONCLUSION

In this study, CsVG membranes were developed from chitosan crosslinked with vanillin and modified with varying concentrations of gelatin (0.5, 0.75 and 1 %). The modified membranes exhibited good adsorption of crystal violet, with the optimum membrane (CsVG2) obtained at a gelatin concentration of 0.75 %. The addition of vanillin and gelatin improved the physical characteristics of the membrane, such as

porosity, swelling and water absorption, in comparison to the pure chitosan membrane. The optimal parameters for dye adsorption were identified as pH 6, a contact time of 80 min, an initial dye concentration of 3 mg/L and a temperature of 298 K, yielding 88 % dye removal.

Adsorption kinetics conformed to a pseudo-second-order model, suggesting that both the contact time and the concentration of the dye influenced the adsorption rate and that chemical interactions occurred between the adsorbent and the adsorbate. The isotherm best fits the Freundlich model, with an R^2 value of 0.9989 at 298 K. The thermodynamic results showed that the adsorption process is exothermic ($\Delta H < 0$) and spontaneous ($\Delta G < 0$).

Overall, the results of this study indicate that the CsVG bioadsorbent membrane has good physicochemical properties and the potential to be developed as an effective, environmentally friendly adsorbent for the removal of crystal violet dye from wastewater. Further research is needed to evaluate the membrane's regeneration and reuse capabilities and to examine its application in more complex wastewater systems.

Acknowledgement. The authors would like to acknowledge the Institute for Research and Community Service, Diponegoro University, for its support through the 2025 research program.

ı æª ı Ø

ı æº—Ø— ûı Ö¹ æ—ßó łŒ œ Œœ Æº—ßŒ œ ¹Øı Êı ł¹ª—ßŒª—ßı øı ß¹œ ı ° Œø—Öı ß¹œ æ— —Øó¹ °–¼ı ‰ö Æ¹‰Œ ł°ı óÖ—ø-ªı ¹øŒÖ

KHABIBIKHABIBI,NABILA AMALIA IZAAZ AANISA | RETNO ARIADILUSIANA

Ddo‘qsl dmsneBgdl hsqx,E‘btksxneSkhdmbdr‘mcM ‘sgdl ‘sbbr,Umhudqdhsxne Dhonmdfnqn,4/164 Sdl ‘q‘mf, Bdmsq‘kI‘u‘,Imcnmdth‘

ł ð|Åµ½Ã-ú|ÇÃÐµ (BV) Ð þ½µ ÇÁÅþ½ ÕÇ ½ þÇ ½ ñðÐíÅµ½ú, ½ Ç®Õ|, ÁÐ ð|®|þÐ ñÇ î |úÇµÁÙ ÅðÐí|ÁÙ þ½í½ ÅÐ ½þÙý ÙÃ|ð½ Ù úÇíÐÁ|ý ÐþÇÅ|ÅµÐý |ý½ ®Õçé ÅúÇ Ð ú|ÅÇþÐ µÇþÅ|ÑÁÇÅµ| ®½ î |úÐ Çðê½Á|®ý Ð. æÕÇé µÇê½ ÅÙ ñÇµðÐÕÃÐ ÐÈ |þ½ÁÃÐ ý ÐµÇíÐ µðÐµý ½Á½ ®½ ÙþÃ½" ½" Ð ÇúÐ ÕÇ Ð |® Çµñ½íÁ|Š úÇí½. ö ÇúÇ ˇ Åµ Ùí|ˇ|, Š|µÇ®½ÁÅþ½ (Br) Õ|Ç½íÅÇðÕÐÁµ ý ÐýÕð½Á½, Ùý ðÐî ÐÁ½ Å½ ú½Á|Ã|ÁÇý (V) | ý Çí|È |þÇú½Á½ î ÐÃ½µ|ÁÇý (G), ð½®ú| Ð Á½ Ð ®½ ½íÅÇðñõ| Ù BV .û |µÇ®½Á/ /ú½Á|Ã|Á ýÐýÕð½Á½ Ð ñÇýÐÚ ½Á½ Å½ î ÐÃ½µ|ÁÇý Ù ð½®Ã|Ñ|µ|ý þÇÁÕÐÁµð½õ| ˇ½ý½, /,4 (BrVG1),/,64 (BrVG1) | 1 % (BrVG3).– ðÇõÐÅ½íÅÇðñõ| Ð Ð |Åñ|µ½Á Ù È ÙÁþõ| ˇ| oH ,úðÐ- ýÐÁ½ þÇÁµ½þµ½, ñÇÑÐµÁÐ þÇÁõÐÁµð½õ| Ð ÕÇ Ð | µÐý ñÐð½µÙðÐ.œ ÐýÕð½Á½ Ð Çþ½ð½þµÐð|Å½Á½ ýÐðÐ" Ðý ñÇðÇ®ÁÇÅµ| ,ÅµÐñÐÁ ‘ ÕÙÕðÐ" ½,½ñíÅÇðñõ| ˇd úÇíÐ, ETIR | SEM .°Ð®ÙÃµ½µ| ÅÙ ñÇþ½- ®½Ã| í½ÅÙ Çñµ|ý½ÃÃ| ñ½ð½ý Ðµð| ®½½íÅÇðñõ| Ù ÕÇ Ð Õ|Ã| oH 6,úðÐý Ð þÇÁµ½þµ½ 8/ l hm | µÐý ñÐð½µÙð½ 198 K,Ú µÇ Ð ðÐ®ÙÃµ|ð½Ã Ùþ Ã½" ½" Ðý 88 % ÕÇ Ð. ł |Áðµ|þ½½íÅÇðñõ| Ð ñð½- µ|Ã½ Ð ýÇíÐÃ ñÅÐÙíÇ-íðÙéÇéðÐí½, ½ Eqdtmcklbbg ýÇíÐÃ Á½ÕÇ, Ð Ð Çñ|Å½Ç |®ÇµÐðý Ù½íÅÇðñ- õ| Ð. ÖÐðýÇí|Á½ý |Ñþ½½Á½Ã|®½ Ð ñÇþ½®½Á½í½ Ð ñðÇõÐÅ½íÅÇðñõ| Ð Õ|Ç Å½ÇÃµ½Á | Ðê®ÇµÐð- ý½Á. Ø½þÃÐ, BrVG ýÐýÕð½Á½ |ý½ ñÇµÐÁõ| ½Ã í½ ñÇÃÃÙî | þ½Ç ÐÈ |þ½ÁÁ½ ½ÃµÐðÃ½µ| ú½ ®½ Ùþ½" ½" Ð þð|Å½Ãç , ÙÕ|Ñ½Åµ Ð |®µÐþÅµ|ÃÁ|Š |ÁíÙÅµð| Åþ|Š Çµñ½íÁ|Š úÇí½.

(– ð|ý , ÐÁÇ 9. ½ÁÙ½ð½, ðÐú|í|ð½ÁÇ 16. ½ÁÙ½ð½, ñð|Šú½» ÐÁÇ 9. ½ñð|Ã½ 1/16)

REFERENCES

1. E. Alver, A. Ü. Metin, *Chem. Eng. J.* **200**–**202** (2012) 59 (https://doi.org/10.1016/j.cej.2012.06.038)
2. M. Greluk, Z. Hubicki, *Desalination* **278** (2011) 219 (https://doi.org/10.1016/j.desal.2011.05.024)
3. C. Ruiz, M. Vera, B. L. Rivas, S. Sánchez, B. F. Urbano, *RSC Adv*. **10** (2020) 43799 (https://doi.org/10.1039/D0RA08188D)
4. A. K. Hady, M. E. Owda, R. E. Abouzeid, H. A. Shehata, A. S. Elzaref, A. S. Elfeky, *Biomass Convers. Biorefinery* **15** (2025) 759 (https://doi.org/10.1007/s13399-023-05146-0)
5. R. Mohammad-Rezaei, B. Khalilzadeh, F. Rahimi, S. Moradi, M. Shahlaei, H. Derakhshankhah, M. Jaymand, *Environ. Res.* **214** (2022) 113966 (https://doi.org/10.1016/j.envres.2022.113966)
6. D. Ordonez, A. Valencia, B. Pereira, N.-B. Chang, *Environ. Res*. **212** (2022) 113208 (https://doi.org/10.1016/j.envres.2022.113208)
7. R. S. Dassanayake, S. Acharya, N. Abidi, *Molecules* **26** (2021) 4697 (https://doi.org/10.3390/molecules26154697)
8. X. Zhao, X. Wang, T. Lou, *J. Hazard. Mater*. **403** (2021) 124054 (https://doi.org/10.1016/j.jhazmat.2020.124054)
9. W. Liu, T. Lou, X. Wang, *Int. J. Biol. Macromol*. **242** (2023) 124711 (https://doi.org/10.1016/j.ijbiomac.2023.124711)
10. C. Miao, W. Huang, K. Li, Y. Yang, *Environ. Res*. **263** (2024) 120195 (https://doi.org/10.1016/j.envres.2024.120195)
11. B. Tomadoni, A. Ponce, M. Pereda, M. R. Ansorena, *Polym. Test*. **78** (2019) 105935 (https://doi.org/10.1016/j.polymertesting.2019.105935)
12. R. Resmi, S. Unnikrishnan, L. K. Krishnan, V. Kalliyana Krishnan, *J. Appl. Polym. Sci*. **134** (2017) (https://doi.org/10.1002/app.44529)
13. D. Mangla, A. Sharma, S. Ikram, *React. Funct. Polym*. **175** (2022) 105261 (https://doi.org/10.1016/j.reactfunctpolym.2022.105261)
14. R. A. Lusiana, N. B. A. Prasetya, K. Khabibi, *Indonesian J. Chem. Sci.* **9** (2020) 194 (https://journal.unnes.ac.id/sju/ijcs/article/view/41759/17209) (In Indonesian)
15. J. Yuan, Z.-Z. Pan, Y. Jin, Q. Qiu, C. Zhang, Y. Zhao, Y. Li, *J. Power Sources* **500** (2021) 229983 (https://doi.org/10.1016/j.jpowsour.2021.229983)
16. U. S. Malik, Q. Duan, M. B. K. Niazi, Z. Jahan, U. Liaqat, F. Sher, Y. Gan, H. Hou, *Chin. Chem. Lett*. **34** (2023) 108071 (https://doi.org/10.1016/j.cclet.2022.108071)
17. B. Farasati Far, M. R. Naimi-Jamal, M. Jahanbakhshi, S. A. Khalafvandi, M. Alian, D. Razeghi Jahromi, *J. Mol. Liq*. **395** (2024) 123839 (https://doi.org/10.1016/j.molliq.2023.123839)
18. N. Parshi, D. Pan, V. Dhavle, B. Jana, S. Maity, J. Ganguly, *Int. J. Biol. Macromol*. **141** (2019) 626–635 (https://doi.org/10.1016/j.ijbiomac.2019.09.025)
19. C. Ye, B. Yan, X. Ji, B. Liao, R. Gong, X. Pei, G. Liu, *Ecotoxicol. Environ. Saf*. **180** (2019) 366–373 (https://doi.org/10.1016/j.ecoenv.2019.04.086)
20. S. El Bourachdi, A. El Amri, A. R. Ayub, F. Moussaoui, Y. Rakcho, F. El Ouadrhiri, A. Adachi, M. Lechheb, J. A. Herrera-Melián, A. Lahkimi, *Int. J. Biol. Macromol*. **305** (2025) 141030 (https://doi.org/10.1016/j.ijbiomac.2025.141030)
21. G. Purwiandono, P. Lestari, *J. Ecol. Eng*. **24** (2023) 137 (https://doi.org/10.12911/22998993/166319)

22. L.-C. Juang, C.-C. Wang, C.-K. Lee, *Chemosphere* **64** (2006) 1920 (https://doi.org/10.1016/j.chemosphere.2006.01.024)
23. S. Jabbarvand Behrouz, A. Khataee, M. Safarpour, S. Arefi-Oskoui, S. Woo Joo, *Sep. Purif. Technol*. **269** (2021) 118720 (https://doi.org/10.1016/j.seppur.2021.118720)
24. S. Wang, H. Wang, S. Wang, L. Fu, L. Zhang, *Sep. Purif. Technol*. **307** (2023) 122783 (https://doi.org/10.1016/j.seppur.2022.122783)
25. H. Yu, Y. Ge, H. Ding, Y. Yan, L. Wang, Int. J. Biol. *Macromol*. **253** (2023) 126726 (https://doi.org/10.1016/j.ijbiomac.2023.126726)
26. S. J. Peighambardoust, S. Imani Zardkhaneh, M. Foroughi, R. Foroutan, H. Azimi, B. Ramavandi, *Environ. Res*. **258** (2024) 119428 (https://doi.org/10.1016/j.envres.2024.119428)
27. G. Michailidou, E. N. Koukaras, D. N. Bikiaris, *Int. J. Biol. Macromol*. **192** (2021) 1266 (https://doi.org/10.1016/j.ijbiomac.2021.10.093)
28. C. Xu, W. Zhan, X. Tang, F. Mo, L. Fu, B. Lin, *Polym. Test*. **66** (2018) 155 (https://doi.org/10.1016/j.polymertesting.2018.01.016)
29. R. L. C. G. da Silva, O. D. Bernardinelli, E. C. G. Frachini, H. Ulrich, E. Sabadini, D. F. S. Petri, *Carbohydr. Polym*. **292** (2022) 119725 (https://doi.org/10.1016/j.carbpol.2022.119725)
30. J. R. Westlake, M. Laabei, Y. Jiang, W. C. Yew, D. L. Smith, A. D. Burrows, M. Xie, *ACS Food Sci. Technol*. **3** (2023) 1680 (https://doi.org/10.1021/acsfoodscitech.3c00222)
31. Z. Zhang, J. Zhao, W. Li, H. Yuan, Y. Chi, J. Tang, J. Wang, Z. Xie, *J. Environ. Chem. Eng.* **13** (2025) 118743 (https://doi.org/10.1016/j.jece.2025.118743)
32. M. Carpintero, I. Marcet, C. Cortizo, P. Guerrero, K. de la Caba, M. Rendueles, M. Díaz, *Food Hydrocoll*. **171** (2026) 111838 (https://doi.org/10.1016/j.foodhyd.2025.111838)
33. Y. Peng, Y. Yu, Z. Su, Y. Zhong, S. Vijayakumar, Y. Chen, Y. Mao, M. Xin, M. Li, *Carbohydr. Polym*. **367** (2025) 124015 (https://doi.org/10.1016/j.carbpol.2025.124015)
34. Y. Yang, Y. Zhang, G. Wang, Z. Yang, J. Xian, Y. Yang, T. Li, Y. Pu, Y. Jia, Y. Li, Z. Cheng, S. Zhang, X. Xu, *J. Environ. Chem. Eng*. **9** (2021) 105407 (https://doi.org/10.1016/j.jece.2021.105407)
35. L. Chen, H.-H. Cheng, J. Xiong, Y.-T. Zhu, H.-P. Zhang, X. Xiong, Y.-M. Liu, J. Yu, Z.-X. Guo, *Chin. J. Polym. Sci*. **36** (2018) 1063 (https://doi.org/10.1007/s10118-018-2112-0)
36. H. Bakouri, A. Ziane, K. Guemra*, Int. J. Biol. Macromol*. **230** (2023) 123181 (https://doi.org/10.1016/j.ijbiomac.2023.123181)
37. F. Mashkoor, A. Nasar, C. Jeong, *Biomass Convers. Biorefinery* **14** (2024) 313 (https://doi.org/10.1007/s13399-021-02282-3)
38. S. Haider, S. Y. Park, S. H. Lee, *Soft Matter* **4** (2008) 485 (https://doi.org/10.1039/b713944f)
39. S. Amjadi, S. Emaminia, S. Heyat Davudian, S. Pourmohammad, H. Hamishehkar, L. Roufegarinejad, *Carbohydr. Polym*. **216** (2019) 376 (https://doi.org/10.1016/j.carbpol.2019.03.062)
40. J. Hu, Z. Wang, J. M. Miszuk, M. Zhu, T. I. Lansakara, A. V. Tivanski, J. A. Banas, H. Sun, *Carbohydr. Polym*. **271** (2021) 118440 (https://doi.org/10.1016/j.carbpol.2021.118440)
41. H. Mittal, A. Al Alili, P. P. Morajkar, S. M. Alhassan, *J. Mol. Liq*. **323** (2021) 115034 (https://doi.org/10.1016/j.molliq.2020.115034)

42. S. A. Ganiyu, M. A. Suleiman, W. A. Al-Amrani, A. K. Usman, S. A. Onaizi, *Sep. Purif. Technol*. **318** (2023) 123765 (https://doi.org/10.1016/j.seppur.2023.123765)
43. S. A. Bahadi, M. Iddrisu, M. K. Al-Sakkaf, M. A. A. Elgzoly, Q. A. Drmosh, W. A. Al-Amrani, U. Ahmed, U. Zahid, S. A. Onaizi, *Emergent Mater*. **7** (2024) 959 (https://doi.org/10.1007/s42247-023-00513-z)
44. H. Jayasantha Kumari, P. Krishnamoorthy, T. K. Arumugam, S. Radhakrishnan, D. Vasudevan, *Int. J. Biol. Macromol*. **96** (2017) 324 (https://doi.org/10.1016/j.ijbiomac.2016.11.077)
45. C. Zhou, S. Lee, K. Dooley, Q. Wu, *J. Hazard. Mater*. **263** (2013) 334 (https://doi.org/10.1016/j.jhazmat.2013.07.047)
46. G. Agbor Tabi, L. Ngouateu Rene Blaise, K. Daouda, A. Naphtali Odogu, A. Aime Victoire, N. Nsami Julius, K. Joseph Mbadcam, *Arab. J. Chem.* **15** (2022) 103515 (https://doi.org/10.1016/j.arabjc.2021.103515)
47. R. Ahmad, M. O. Ejaz, *Dyes Pigments* **216** (2023) 111305 (https://doi.org/10.1016/j.dyepig.2023.111305)
48. A. Salah Omer, G. A.El Naeem, A. I. Abd-Elhamid, O. O.M. Farahat, A. A. El-Bardan, H. M.A. Soliman, A. A. Nayl, *J. Mater. Res. Technol*. **19** (2022) 3241 (https://doi.org/10.1016/j.jmrt.2022.06.045)
49. L. Liu, Z. Y. Gao, X. P. Su, X. Chen, L. Jiang, J. M. Yao, *ACS Sustain. Chem. Eng*. **3** (2015) 432 (https://doi.org/10.1021/sc500848m).